RSC Advances

ROYAL SOCIETY OF CHEMISTRY

www.rsc.org/advances

A disposable paper-based electrochemiluminescence device for ultrasensitive monitoring of CEA based on $Ru(bpy)_3^{2+}$@Au nanocages

Chaomin Gao[a], Min Su[a], Yanhu Wang[a], Shenguang Ge[b], Jinghua Yu[a]*

[a] *Key Laboratory of Chemical Sensing & Analysis in Universities of Shandong, School of Chemistry and Chemical Engineering, University of Jinan, Jinan 250022 (P. R. China)*

[b] *Shandong Provincial Key Laboratory of Fluorine Chemistry and Chemical Materials, University of Jinan, Jinan 250022 (P.R. China)*

*Corresponding authors: Jinghua Yu

E-mail: ujn.yujh@gmail.com

Telephone: +86-531-82767161

ABSTRCT

In this work, an electrochemiluminescence (ECL) immunoassay integrated with the proposed 3D microfluidic origami device for the sensitive detection of carcinoembryonic antigen (CEA) was developed based on Ag nanospheres modified paper working electrode (Ag-PWE) as sensor platform and Au nanocages functionalized tris-(bipyridine)-ruthenium(II) ($Ru(bpy)_3^{2+}$) as the ECL signal amplification label. The novel Ag-PWE with excellent conductivity was constructed through the growth of an Ag nanospheres layer on the surfaces of cellulose fibers and served to provide a good pathway for electron transfer and enhance the amount of capture antibody (Ab_1). Au nanocages, which possessed a hollow structure, were first used to construct the ECL immunosensor as a signal amplification carrier. In both the inner and outer surfaces of the Au nanocages can adsorb $Ru(bpy)_3^{2+}$, therefore, the signal can be amplified as much as possible. In addition, this as-prepared 3D microfluidic origami ECL immunodevice had the advantages of high sensitivity, acceptable precision and reasonable accuracy. On the basis of the considerably amplified ECL signal and sandwich-type format, the as-proposed immunodevice successfully fulfilled the highly sensitive detection of CEA with a linear range 0.001-50 $ngmL^{-1}$ and a detection limit of 0.0007 $ng{\cdot}mL^{-1}$. The resulting 3D microfluidic origami ECL immunodvice exhibited great promise in the point-of-care diagnostics application of clinical screening of tumor markers.

1. Introduction

Tumor markers are molecules that occur in blood and tissues associated with cancer, whose identification and determination is useful in patient diagnosis and clinical therapy [1]. Carcinoembryonic antigen (CEA), a polysaccharide-protein complex, is widely considered as a clinical tumor marker, and it has been evaluated in a wide range of malignancies, such as

colorectal cancer, pancreatic cancer, and liver cancer, and its levels may reflect the disease progression or regression status [2]. Therefore, the development of an ultrasensitive and simple method for the determination of CEA is of great importance. Immunoassay, based on the mechanism of specific antibody-antigen interactions, is one of the most important methods for the specific detection of tumor markers because complex separation and extraction steps are essentially avoided and their specificity, analytical time and practicability are enhanced [3]. Until now, immunoassays, including radioimmunoassays [4-5], enzyme-linked immunosorbent assay (ELISA) [6-7], chemiluminescence immunoassay (CLIA) [8-9] and piezoelectric immunosensors [10-11] have been widely reported for tumor markers detection. However, most of the above mentioned methods usually remain cumbersome, time-consuming, and harmful to the operator health.

Electrochemiluminescence (ECL), which combines the electrochemical and luminescent techniques, is a light emission process in a redox reaction of electrogenerated reactants [12]. Compared with the conventional electrochemical immunoassays, the ECL immunoassay has become one of the predominant analytical techniques for its intrinsic advantages such as fast response time, simple instrumentation, wide dynamic concentration response range and excellent detection sensitivity during the past several decades. Thence, the ECL immunoassay which integrated the high specificity of immunoassay and the high sensitivity of electrochemical has become a powerful analytical tool for highly sensitive and specific detection of clinical samples [13-16].

Since microfluidic paper-based analytical devices (μ-PADs) were firstly proposed by Whitesides' group [17], μ-PADs were considered to be an ideal point-of-care (POC) diagnostic

platforms for developing countries, resource-limited and remote regions, because they have attractive features including low cost, ease of use, low consumption of reagent and sample, portability and disposability [18-21]. Compared with other organic or inorganic materials, paper has several additional advantages for electronic devices fabrication [22]. As one of the most important inventions, Paper is already utilized extensively as a platform in analytical and clinical chemistry. Paper is a ubiquitous material composed mainly of cellulose that is inexpensive, easy to manipulate, biodegradable or easily disposable by incineration and compatible with several biological and chemical assays [23], which make it possible to pattern hydrophilic channels separated by hydrophobic walls of photoresist/polymer, ink, wax, and plasma treatment, laser treatment or by cutting method. Recently, μ-PADs have drawn considerable attention and been regarded as a promising method for tumor marker detection. The establishment of ECL on μ-PADs [24] based on the integration of μ-PADs and screen-printed electrodes have substantially increased the scope of options for detections and shown excellent prospects for analytic detection. To perform high-performance, sensitive-enhanced sandwich-type ECL immunoassays, much attention have been focused on signal amplification processes. In this present work, Ruthenium(II) tris(2,2′-bipyridyl) ($Ru(bpy)_3^{2+}$) was used as ECL luminophore due to its advantages in chemical stability, reversible electrochemical behavior, and luminescence efficiency over a wide range of buffer pH levels [25-26]. To enhance the luminous intensity of the $Ru(bpy)_3^{2+}$-based ECL system, lots of groups spare no efforts to find the appropriate signal amplification carrier. With the goal of obtaining the desirable carrier, we successfully synthesize the Au nanocages and use them as the signal amplification carrier. The Au nanocages have a hollow structure, which could provide a large room for $Ru(bpy)_3^{2+}$ and are superior in terms of high surface-to-volume and good stability.

In this work, we successfully designed a sensitive sandwich-type ECL immunosensor for accurate determination of CEA by developing a 3D μ-PADs which is based on the Ag-PWE as sensor platform and $Ru(bpy)_3^{2+}$@Au nanocages as signal amplification label. The low cost and portable 3D μ-PADs were constructed directly by screen-printing carbon working, counter electrodes and Ag/AgCl reference electrode including their conductive pads on wax-patterned pure cellulose paper, and were activated by folding to form a 3D electrochemical cell. To construct the Ag-PWE, a continuous and dense Ag NPs layer was grown on the surfaces of cellulose fibers in the paper sample zone. It was the porous structure of paper as well as the high conductivity of Ag nanospheres that made the active surface area and the sensitivity of this Ag-PWE much higher than that of unmodified PWE. The as-synthesized $Ru(bpy)_3^{2+}$@Au nanocages were serviced as signal amplification platform to load more signal antibody (Ab_2). With a folding procedure, the as-prepared 3D μ-PADs were added into a home-made device-holder and ready for CEA detection. The aim of our study is to explore simple, sensitive, low-cost and portable point-of-care testing devices.

2. Experimental

2.1. Reagents and materials

Deionized water obtained from a Millipore water purification system (>18.2 MΩ.cm, Milli-Q, Millipore) was used in all assays and solutions. All chemicals were commercially available and of analytical grade. Carcinoembryonic antigen (CEA), mouse monoclonal capture antibodies (Ab_1), and signal antibodies (Ab_2) were purchased from Linc-Bio Science Co. Ltd. (Shanghai, China) and used without further purification. The clinical serum samples were obtained from Shandong Tumor Hospital (All experiments were carried out in compliance with the relevant laws and

institutional guidelines issued by the Ethical Committee of jinan University. And the experiments were also approved by the Ethical Committee of jinan University). Bovine serum albumin (BSA), Tetrachloroauric acid ($HAuCl_4$), $NaBH_4$, trisodium citrate glucose, Poly(Vinyl pyrrolidone) (PVP, MW 40,000), sodium citrate, ammonia solution (28 wt %) and sodium carbonate were obtained from Shanghai Chemical Reagent Corporation (Shanghai, China) and used as received. Phosphate-buffered saline (PBS, 10.0 mM) with different pH values were prepared with KH_2PO_4 and Na_2HPO_4. PBS (0.1 M, pH 7.4) was used as the electrolyte in the measuring system. The washing buffer was PBS (pH 7.4, 10.0 mM) containing 0.05% (w/v) Tween-20. PBS (pH 7.4, 10.0 mM) was used as blocking solution. Whatman chromatography paper # 2 (58.0 cm × 68.0 cm) (pure cellulose paper) was obtained from GE Healthcare Worldwide (Pudong, Shanghai, China) and used with further adjustment of size (A4 size). Carbon ink (ELECTRODEDAGPF-407C) and Ag/AgCl ink (ELECTRODAG7019 (18DB19C)) were purchased from Acheson (Germany).

2.2 Apparatus

All electrochemical immunoassays were performed on a CHI 760D electrochemical workstation (Chenhua, Shanghai, China). The scanning electron microscopy (SEM) images were taken by QUANTA FEG 250 thermal field emission scanning electron microscopy (FEI Co., USA).

2.3 Preparation of the 3D microfluidic origami ECL immunodevice

In this paper, wax was used as the paper hydrophobization and insulation agent. Cellulose paper was used to fabricate the 3D μ-PADs, and the fabrication process took very little time. The details were depicted as follows: firstly, the shape of hydrophobic barrier on this origami immunodevice was designed using Adobe illustrator CS4 (Fig. S1), and a wax printer was used for

wax-patterning in bulk (Fig. S2). Secondly, the wax-patterned paper sheet was baked in an oven at 130 °C for 150 s to let wax sufficiently melt and penetrate through the pattern to form the hydrophobic and insulating patterns (Fig. S3). The wax-patterned paper sheet was then ready for screen-printing of electrode array on its paper electrochemical cell after cooling to room temperature. This 3D microfluidic origami ECL immunodevice constituted two sides of one patterned cellulose paper of the size. In paper-A, carbon ink was used for screen-printing working electrode (4.0 mm in diameter); in paper-B, carbon ink and Ag/AgCl ink were used for screen-printing half-ring like counter electrode and reference electrode, respectively (Fig. S4). Sequentially, the wax-patterned paper sheet was cut to Paper-A and Paper-B (Scheme 1).

2.4 Preparation of the Ag-PWE

The Ag-PWE was obtained through growth of an Ag NPs layer which served to enhance the conductivity and enlarge the effective surface area of PWE on the surfaces of cellulose fibers in the paper sample zone of PWE. The overall procedure consists of two processes. Firstly, an Au nanospheres layer on the surfaces of cellulose fibers in the PWE was obtained and the process can be depicted as follows: Firstly, the suspension of AuNP seeds was prepared by using $NaBH_4$ as the reductant and stabilized with sodium citrate according to the literature [27]. Then an amount of 30.0 μL of above AuNP seeds solution was dropped into the bare PWEs and the origami device was then equilibrated at room temperature for 1 h so that more AuNP seeds were fixed on cellulose fibers. After the end of the equilibration time the origami device was washed with deionized water thoroughly according to the literature [28] to remove loosely bound AuNP seeds. After that, freshly prepared AuNP-growth solution (15.0 μL) of PBS (pH 7.4, 10.0 mM) containing $HAuCl_4$ (1.2 mM), cetyltrimethylammonium chloride (2.0 mM) and H_2O_2 (7.2 mM)

for seeds growth was applied into the AuNP seeded PWEs, respectively, and incubated at room temperature for 10 min. According to the literature [29] the AuNP seeds acted as catalysts for the reduction of $AuCl_4^-$ by H_2O_2 during the growth process, resulting in the enlargement of the AuNP seeds. Finally, the resulting AuNPs modified PWEs were rinsed thoroughly with deionized water.

Then, 15.0 μL of freshly prepared Ag-growth solution containing 2.0 mM $AgNO_3$ and 20.0 mM AA was added into the AuNP seeded PWEs, respectively, and incubated at room temperature for 5 min. Finally, the resulting Ag-PWE was washed extensively with deionized water and dried at room temperature for 20 min.

2.5 Preparation of the Au nanocages and $Ru(bpy)_3^{2+}$@Au nanocages labeled signal Ab_2

Au nanocages were obtained according to the recently reported [30] with some modification. To prepare the Au nanocages, Cu_2O cube precursors were first synthesized. In brief, 1 mL mixed solution consisting of 0.74 M sodium citrate and 1.2 M sodium carbonate was added to a round-bottomed flask containing 18.0 mL solution of 0.038 M $CuSO_4$, followed by adding 3.5 g PVP and stirred vigorously until PVP was dissolved completely. Then the round-bottomed flask was transferred to an oil bath at 80 °C and aged for 2 h. After that, the brick-red products were formed and collected. At room temperature, the Cu_2O cube precursors were dispersed in 8.0 mL 0.5 % PVP aqueous solution. Then the solution was diluted with deionized water to 19.5 mL, followed by adding 2.4 mL 10.0 mM $HAuCl_4$ solution under vigorous stir, black precipitate formed immediately. After 6 h, the black precipitate was collected and dispersed in 40.0 mL solution containing 0.04 % PVP and 1 % ammonia for about 12 h. The precipitate was then separated and re-dispersed in 40.0 mL solution containing 0.04 % PVP and 1 % ammonia again for another 12 h. At last, the precipitate was collected by centrifugation, washed with deionized water and dried

under vacuum overnight.

$Ru(bpy)_3^{2+}$ labeled Ab_2 were prepared according to the article with slight modifications [31] Firstly, 80.0 μg $Ru(bpy)_3^{2+}$-NHS ester predissolved in 1.5 μL dimethylsulfoxide (DMSO) to 50.0 μL of Ab_2 at 1 $mg \cdot mL^{-1}$. Then the mixture was filtered through a Sephadex G-25 PD-10 desalting column and eluted with PBS (pH 7.4) after incubation at room temperature in the dark for 40 min. Finally, the purified $Ru(bpy)_3^{2+}$-labeled Ab_2 were further diluted with PBS (pH 7.4) to 1.0 mL and stored at 4 °C environment until use.

The $Ru(bpy)_3^{2+}$-labeled Ab_2 was dispersed in PBS (pH 7.4) to a final volume of 2.0 mL. Then the $Ru(bpy)_3^{2+}$-labeled Ab_2 was mixed with 1.0 mL of as-prepared Au nanocages and stirred for 4 h. Subsequently, the mixture was centrifuged and washed with deionized water several times. Finally, the Au nanocages@$Ru(bpy)_3^{2+}$-labeled Ab_2 was successfully obtained.

2.6 Preparation of the 3D microfluidic origami ECL immunodevice

As shown in Scheme 2, the construction process can be described as follows: 5.0 μL of Ab_1 (20 $\mu g \cdot mL^{-1}$) was dropped onto the corresponding Ag-PWE, and incubated for 40 min. Subsequently, PBS was used to remove the excess antigen. Then 5.0 μL of BSA blocking solution was applied to above Ag-PWE and incubated for 40 min at room temperature to block possible remaining active sites against nonspecific adsorption, and allowing the working electrode to dry for 15 min under ambient conditions. After another washing with washing buffer, the resulting 3D microfluidic origami ECL immunodevice was successfully obtained and stored at 4 °C in a dry environment prior to use.

2.7 ECL assay procedure of this 3D microfluidic origami ECL immunodevice

The ECL assay procedures of this 3D microfluidic origami ECL immunodevice were shown

in Scheme 2, and the detailed procedures were described as follows: briefly, the modified Ag-PWE was incubated with 5.0 μL of CEA standard solution with a series of concentrations for 30 min at room temperature, followed by washing with washing buffer. Then 5.0 μL of the $Ru(bpy)_3^{2+}$@Au nanocages labeled Ab_2 (10 $\mu g \cdot mL^{-1}$) was added to corresponding working electrodes, and incubated for 30 min at room temperature, followed by washing with washing buffer.

Then, as can be seen from the Scheme 1, the folding processes can be described as follows: the sample tab was folded down below the auxiliary pad successively and clamped into the device-holder, which was comprised of two circuit boards (named Board-A and Board-B respectively below) with conductive pads on them, to fix and connect this 3D microfluidic origami ECL immunodevice to the electrochemical workstation [32]. Thereafter, 40.0 μL of PBS solution (pH 7.4,) containing 5.0×10^{-6} mol L^{-1} TPA was added through the hole on board B (Scheme 2), and the as-prepared origami ECL immunodevice was ready for CEA detection. Cyclic voltammetry measurements were carried to touch off the ECL reaction, with the sweeping range from 0 to 1.2 V and a scan rate of 100 mV s^{-1} at room temperature. The ECL emission was detected using the PMT, which biased at 800 V. By analyzing the ECL signals related to the CEA concentrations, CEA could be detected.

3. Results and discussion

3.1 Characterization of Ag-PWE

The continuous porous Ag-PWE was fabricated by growing an Ag NPs layer on the surfaces of cellulose fibers in paper sample zone. The bare paper working zone possessed high ratio of surface area could provide a fine adsorption capability for the Au NPs seeds. As shown in Fig. 1A,

B, C, a continuous and dense Ag NPs conducting layer on the cellulose fiber surfaces in paper sample zone was observed. With the growth time increasing, the Ag NPs were rapidly enlarged by incubating in the growth solution, which indicated that a good coverage of Ag NPs on the surfaces of the PWE was obtained.

In addition, as can be seen from the Fig. 1, the Ag-PWE modified still maintained good porous structure after the growth process, which would benefit the further antibodies modification and analytical application.

3.2 Characterization of Cu_2O and Au nanocages

Typical SEM images of the as-prepared Cu_2O and Au nanocages are given in Fig. 2. To indicate that the Au nanocages consist purely of well-defined cubes with a diameter distribution of about 200-300 nm. The size and morphology distribution of the Au nanocages (Fig. 2B) agrees with that of Cu_2O templates (Fig. 2A). Fig. 2C depicts the EDS of the Au nanocages and also confirms the successful preparation of Au nanocages.

3.3 Optimization of experimental conditions

In order to obtain optimum ECL response, a series of experiments were conducted to select optimal analytical conditions. As we all know, the highly acidic or alkaline environment was not conducive to the activity of the protein and would affect the absorbance of Ab_1 on the surface of Ag-PWE and then affect the immunoreaction of antibody-antigen. Therefore, proper pH environment is very important. We investigated the effect of pH from 6.0 to 8.5 (Fig. 3A). As shown in Fig. 3A, the ECL response gradually increased from pH 6.0 to pH 7.4 and then rapidly decreased at pH values higher than 7.4. Accordingly, the PBS solution of pH 7.4 was chosen for further ECL detection.

In addition, the incubation time was another important parameter affecting the immunoreaction. The effects of incubation time on the ECL intensity of this 3D microfluidic origami ECL immunodevice were investigated as follows. The effect of incubation time was investigated between 20 and 50 min. As shown in Fig. 3B, with an increasing incubation time, the ECL intensities for CEA increased quickly and reached their maximum values at 35 min, thus, an incubation time of 35 min was selected in the further study.

3.4 Analytical performance of the proposed ECL immunosensors.

The Fig. 4A is the ECL signal-time curve under continuous potential scanning for 9 cycles. As can be seen from the figure, the stability of paper-based analytical sensor evaluated with a workstation, which did not appear obvious changes in the ECL intensity. As expected, the ECL intensity in the presence of CEA (curves b-h) was higher than that in the absence of CEA (curve a), and increased gradually with increasing concentrations of CEA (Fig. 4B).

The effectiveness of the as-prepared origami ECL immunodevice was characterized by its analytical performance. The standard calibration curve (Fig. 4C) was obtained by testing a series of concentrations of CEA antigen. As shown in Fig. 4C, the ECL intensity increased linearly with the CEA concentration from 0.001-50 ngmL^{-1}. The linear regression equation is I=458.6 lg c + 1707.6 (where I is the ECL intensity and c represents the concentration of CEA), with the correlation coefficient of R=0.9978. The limit of quantification, according to the definition of a signal-noise ratio of 3, was 0.0007 ng·mL^{-1}, which was much lower than the reported methods [33-36].

3.5 Reproducibility, stability, and specificity.

For the as-prepared 3D microfluidic origami ECL immunodevice, the reproducibility of the

proposed origami ECL immunodevice was evaluated. To evaluate the inter-assay precision, six immunodevice prepared independently following the same experimental protocols were used for the detection of 10.0 ng·mL^{-1} CEA. The obtained variation coefficients were 5.2 %. A series of six immunodevice prepared from the same batch were used to evaluate the intra-assay precision at a concentration level of 10.0 ng·mL^{-1}, the obtained variation coefficients were 4.7 %. The stability of immunodevice array was also examined. The origami ECL immunodevice, which has stored at 4 ℃ in a refrigerator for over two months was used to detect the same concentration of CEA. The ECL intensity of the 3D microfluidic origami ECL immunodevice was still retained at 93 % value of the initial response, which indicated a quite excellent stability.

Specificity is an important criterion for the as-prepared immunodevice. Some coexisting species including AFP (1.0 ng·mL^{-1}), PSA (1.0 ng·mL^{-1}), and HSA (1.0 ng·mL^{-1}) were used as the foreign species to assess the specificity. When 1.0 ng·mL^{-1} AFP, PSA, and HSA were incubated, respectively, the ECL signals were almost the same as the background current. When CEA coexisted with 1.0 ng·mL^{-1} AFP, 1.0 ng·mL^{-1} PSA or 1.0 ng·mL^{-1} HSA, no apparent signal change took place in comparison with the only CEA existed in the buffer. However, the ECL signal of buffer with CEA was tremendously higher than buffer without CEA.

3.6 Analysis of real samples.

To evaluate the applicability of this ECL immunoassay for testing real samples, four serum samples obtained from Shandong Cancer Hospital were measured by the proposed ECL immunosensors as well as the reference commercial ECL method. Prior to detection, the serum samples were diluted appropriately step by step until the concentration of samples reached the linear range of the as-prepared immunodevice. The test results are listed in Table 1, compared with

the reference values, the relative deviations were no more than 3.43 %, indicating an acceptable accuracy. Based on the above results, the as-proposed 3D origami ECL immunodevice could be anticipated to rapidly detect CEA levels in clinical diagnosis.

3.7 Possible mechanism for the ECL behavior of the system

ECL, involving a light emission process in a redox reaction of electrogenerated reactants, combines the electrochemical and luminescent techniques. It involves the production of reactive intermediates from stable precursors at the surface of an electrode. These intermediates then react under a variety of conditions to form excited state that emit light.

Therefore, this $Ru(bpy)_3^{2+}$-TPA ECL system could be used for the sensitive determination of K562 cancer cells. These ECL characterizations were in agreement with published work and its mechanism is presented below [35]:

$$Ru(bpy)_3^{2+} - e^- \rightarrow Ru(bpy)_3^{3+} \quad (1)$$

$$TPA - e^- \rightarrow [TPA^{\bullet}]^+ \rightarrow TPA^{\bullet} + H^+ \quad (2)$$

$$Ru(bpy)_3^{3+} + TPA^{\bullet} \rightarrow Ru(bpy)_3^{2+}* + \text{products} \quad (3)$$

$$Ru(bpy)_3^{2+}* \rightarrow Ru(bpy)_3^{2+} + h\nu \quad (4)$$

4. Conclusion

In this work, a 3D microfluidic origami ECL immunodevice was fabricated for CEA detection based on continuous porous Ag-PWE as sensor platform and Au nanocages functionalized tris-(bipyridine)-ruthenium(II) ($Ru(bpy)_3^{2+}$) as signal amplification label. This 3D microfluidic origami ECL immunodevice was fabricated by wax printing, which is rapid, inexpensive and insulative. The Ag-PWE was constructed through the growth of Ag NPs on the surfaces of cellulose fibers. The experimental results indicated that the as-prepared Ag-PWE was

provided with salient conductivity, extraordinary electron transport properties and a very large specific surface area, which led to a very high ECL intensity. The sandwiched ECL immunosensor used functionalized $Ru(bpy)_3^{2+}$@Au nanocages composite as an ideal label and ECL reagent, which has salient labeling property and ECL activity with amplification techniques. The as-proposed cube Au nanocages possessed a high surface-to-volume ratio and were conducive to high loading of $Ru(bpy)_3^{2+}$, as well as the improved electron transport properties. Taking advantages of dual signal amplification effects of the Ag-PWE and $Ru(bpy)_3^{2+}$@Au nanocages, the as-proposed method revealed a wide linear range and excellent reproducibility, precision, and specificity. This as-proposed 3D microfluidic origami ECL immunodevice with a rapid, sensitive and stable ECL response to trace of analyte in real biological samples will be very helpful when the level of analyte in whole blood samples is very important for point-of-care testing in remote regions, developing, or developed countries.

Acknowledgments

This work was financially supported by National Natural Science Foundation of People's Republic of China (No. 21175058 21475052); Natural Science Foundation for Young Scientists of China (Grant No.51003039). Technology Development Plan of Shandong Province, China (Grant No. 2014GGX103012).

References

[1] J. Tang, D.P. Tang, R. Niessner, G.N. Chen, and D. Knopp, Magneto-controlled graphene immunosensing platform for simultaneous multiplexed electrochemical immunoassay using distinguishable signal tags. Analytical Chemistry 2011, 83, 5407-5414

[2] Q.L Yu, X. W, and Y.X D, Capillary-based three-dimensional immunosensor assembly for

high-performance detection of carcinoembryonic antigen using laser-induced fluorescence spectrometry. Analytical Chemistry 2014, 86, 1518-1524.

[3] Q.L Yu, X.F Zhan, K.P Liu, H. Lv, and Y.X Duan, Plasma-enhanced antibody immobilization for the development of a capillary-based carcinoembryonic antigen immunosensor using laser-induced fluorescence spectroscopy. Analytical Chemistry 2013, 85, 4578-4585.

[4] Q. Zhang, Q. Xiao, Z. Lin, X. Ying, Z. Li, J.M. Lin, Development a competitive radiommunoassay for glypican-3 and clinical application in diagnosis of hepatocellular carcinoma. Clinical Biochemistry 2010, 43, 1003-1008.

[5] V. Ledecky, A. Valencakova-Agyagosova, J. Lepej, Z. Frischova, S. Hornak, V. Nagy, Determination of carcinoembryonic antigen and cancer antigen values with the radioimmunoassay method in healthy females dogs. Veterinarni Medicina 2013, 58, 277-283.

[6] S. Lai, S.N. Wang, J. Luo, L.J. Lee, S.T. Yang, M.J. Madou, Design of a compact disk-like microfluidic platform for enzyme-linked immunosorbent assay. Analytical Chemistry 2004, 76, 1832-1837.

[7] E. M. Thurman, Michael Meyer, Michael Pomes, Charles A. Perry, and A. Paul Schwab, Enzyme-linked immunosorbent assay compared with gas chromatography/mass spectrometry for the determination of triazine herbicides in deionized water. Analytical Chemistry 1990, 62, 2043-2048.

[8] S. Bi, H. Zhou, S. Zhang, Multilayers enzyme-coated carbon nanotubes as biolabel for ultrasensitive chemiluminesence immunoassay of cancer biomarker. Biosensors and Bioelectronics 2009, 24, 2961-2966.

[9] L.X Zhao, J.M. Lin, Z.J. Li, X.T. Ying, Development of a highly sensitive, second antibody

format chemiluminescence enzyme immunoassay for the determination of 17 β-estradiol in waste water. Analytica Chimica Acta 2006, 558, 290-295.

[10] J. Zhou, N. Gan, T. Li, H. Zhou, X. Li, Y. Cao, L. Wang, W. Sang, F. Hu, Ultratrace detection of C-reactive protein by a piezoelectric immunosensor based on Fe_3O_4@SiO_2 magnetic capture nanoprobes and HRP-antibody co-immobilized nanogold as signal tags. Sensors and Actuators, B 2013, 178, 494-500.

[11] N.A. Karaseva, T.N. Ermolaeva, A piezoelectric immunosensor for chloramphenicol detection in food. Talanta 2012, 93, 44-48.

[12] M. M. Richter, Electrochemiluminescence (ECL). Chemical Reviews 2004, 104, 3003-3036.

[13] A.J. Bard, Electrogenerated Chemiluminescence. Marcel Dekker: New York 2004.

[14] M.M. Richter, Electrochemiluminescence (ECL). Chemical Reviews 2004, 104, 3003-3036.

[15] C.A. Marquette, L.J. Blum. State of the art and recent advances in immunoanalytical systems. Biosensors and Bioelectronics 2006, 21, 1424-1433.

[16] P Bertoncello, R.J. Forster, Nanostructured materials for electrochemiluminescence (ECL)-based detection methods: recent advances and future perspectives. Biosensors and Bioelectronics 2009, 24, 3191-3200.

[17] A.W. Martinez, S.T. Phillips, M.J. Butte and G.M. Whitesides, Angewandte Chemie International Edition, Patterned paper as a platform for inexpensive, low-volume, portable bioassays 2007, 46, 1318-1320.

[18] A. W. Martinez, S. T. Phillips, G. M. Whitesides, and E. Carrilho, “Diagnostics for the developing world: microfluidic paper-based analytical devices”. Analytical Chemistry 2010, 82, 3-10.

[19] R. Mukhopadhyay, Cheap, handheld colorimeter to read paper-based diagnostic devices. Analytical Chemistry 2009, 81, 8659-8659.

[20] S.K. Sia and L.J. Kricka, Microfluidics and point-of-care testing. Lab on a Chip 2008, 8, 1982-1983.

[21] R. Mukhopadhyay. When microfluidic devices go bad. Analytical Chemistry 20085, 1, 429-432.

[22] L.G Zhang, M. Zhou, D. Wen, L. Bai, B.H Lou, S.J Dong, Small-size biofuel cell on paper. Biosensors and Bioelectronics 2012, 35, 155-159.

[23] Ana M. M. Rosa, A. Filipa Louro, Sofia A. M. Martins, Joã o Iná cio, Ana M. Azevedo, and D. Miguel F. Prazeres, Capture and Detection of DNA Hybrids on Paper via the Anchoring of Antibodies with Fusions of Carbohydrate Binding Modules and ZZ-Domains. Analytical Chemistry 2014, 86, 4340-4347

[24] J.X Yan, L. Ge, X.R Song, M. Yan, S.G Ge, and J.H Yu, Paper-based electrochemiluminescent 3D immunodevice for lab-on-paper, specific, and sensitive point-of-care testing. Chem. Eur. J 2012, 18, 4938-4945.

[25] Z.H. Chen, Y. Liu, Wang, Y.Z. Wang, X. Zhao, J. H. Li, Dynamic evaluation of cell surface N−glycan expression via an electrogenerated chemiluminescence biosensor based on concanavalin A−integrating gold-nanoparticle-modified $Ru(bpy)_3^{2+}$-doped silica nanoprobe. Analytical Chemistry 2013, 85, 4431-4438.

[26] L.Z. Hu, G.B. Xu, Applications and trends in electrochemiluminescence. Chemical Society Reviews 2010, 39(8), 3275-3304.

[27] W.P Li H.M Yang C. Ma L. Li S.G Ge X.R Song J.H Yu M. Yan, Electrochemiluminescence

of peroxydisulfate using flower-like Ag@Au-paper electrode and Pd@Au-assisted multiple enzymatic labels. http://dx.doi.org/doi:10.1016/j.electacta.2014.06.130.

[28] J.X. Yan, L. Ge, X.R. Song, M. Yan, S.G. Ge and J.H. Yu, Paper-based electrochemiluminescent 3D immunodevice for lab-on-Paper, specific, and sensitive point-of-care testing. Chemistry A European Journal 2012, 18, 4938-4945.

[29] M. Zayats, R. Baron, I. Popov and I. Willner, Biocatalytic growth of Au nanoparticles: from mechanistic aspects to biosensors design. Nano Letters 2005, 5, 21-25.

[30] X.L Chai, X.G Zhou, Anwei Zhu, Limin Zhang, Yao Qin, Guoyue Shi, and Yang Tian, A two-channel ratiometric wlectrochemical biosensor for in vivo monitoring of copper ions in a rat brain using gold nanocages. Angew. Chem. Int. Ed 2013, 52, 8129-8133.

[31] G. A. Crespo, G. Mistlberger, E. Bakker, Electrogenerated chemiluminescence for potentiometric sensors, Journal of the American Chemical Society 2012, 134, 205-207.

[32] C. Ma, W.P Li, Q.K Kong, H.M Yang, Z.Q Bian, X.R Song, J.H Yua, M. Yan, 3D origami electrochemical immunodevice for sensitive point-of-care testing based on dual-signal amplification strategy. Biosensors and Bioelectronics 2015, 63, 7-13.

[33] S.W. Wang, Y. Zhang, J.H. Yu, X.R. Song, S.G. Ge, M. Yan, Application of indium tin oxide device in gold-coated magnetic iron solid support enhanced electrochemiluminescent immunosensor for determination of carcinoma embryonic antigen. Sensors and Actuators B: Chemical 2012, 171-172, 891-898.

[34] B.J. Jeong, R. Akter, O.H. Han, C.K. Rhee, M.A. Rahman, Increased electrocatalyzed performance through dendrimer-encapsulated gold nanoparticles and carbon nanotube-assisted multiple bienzymatic labels: highly sensitive electrochemical immunosensor for protein detection.

Analytical Chemistry 2013, 85, 1784-1791.

[35] S.W. Wang, L. Ge, Y. Zhang, X.R. Song, N.Q. Li, S.G. Ge, J.H. Yu, Battery-triggered microfluidic paper-based multiplex electrochemiluminescence immunodevice based on potential-resolution strategy. Lab on a chip 2012, 12, 4489-4498.

[36] F.Y. Kong, B.Y. Xu, Y. Du, J.J. Xu, H.Y. Chen, A branched electrode based electrochemical platform: towards new label-free and reagentless simultaneous detection of two biomarkers. Chemical Communications 2013, 49 1052-1054.

[37] L.H. Zhang and S.J. Dong, Electrogenerated Chemiluminescence Sensors Using Ru(bpy)32+ Doped in Silica Nanoparticles, Analytical Chemistry 2006, 78, 5119-5123.

Figure caption

Fig.1 (A-C) Enlarged Au on the surfaces of cellulose fibers in paper sample zone of PWE under different magnification after 5 min of growth.

Fig.2 SEM image of (A) Cu_2O cubic; SEM image of (B) Au nanocages

Fig.3. (A) the ECL intensity of 0.1 $ng \cdot mL^{-1}$ of CEA in different PBS. (B) the ECL intensity of 0.1 $ng \cdot mL^{-1}$ of CEA in pH 7.4 PBS with different incubation time.

Fig.4. (A) ECL emission of the 3D origami ECL immunodevice under continuous CVs for 9 cycles (using 0.1 $ng \cdot mL^{-1}$ CEA as an example). (B) ECL emission of the 3D origami ECL immunodevice in the presence (a-h) of different concentration of PSA and PSA concentration (ng mL^{-1}) was (a) 0.00, (b) 0.001, (c) 0.01, (d) 0.05, (e) 0.1, (f) 5, (g) 50, (h) 100. (C) Relationship between ECL signal and antigen concentration for CEA (the voltage of the photomultiplier tube was set at 800 V, Scan rate, 100 $mV \cdot s^{-1}$.). Inset: logarithmic calibration curve.

Table caption

Table 1. Detection results of serum samples by the proposed and reference method.

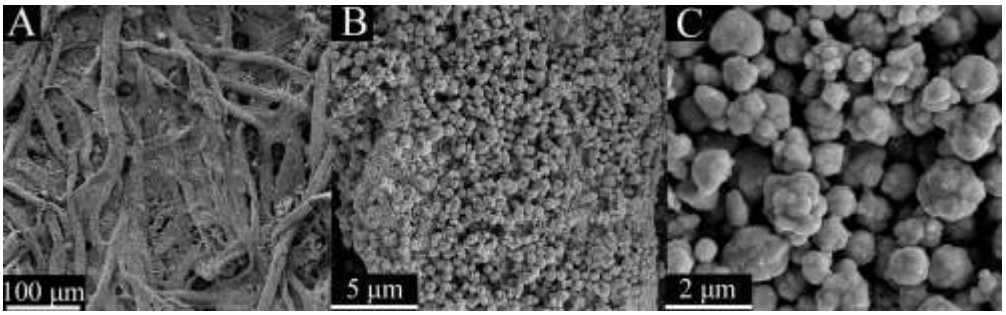

Fig. 1

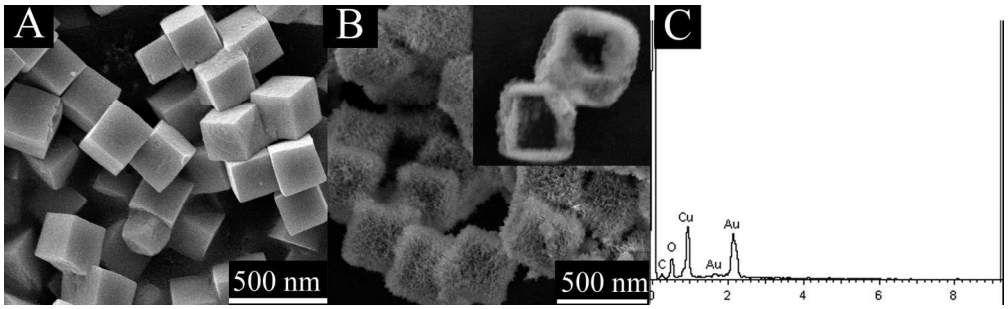

Fig. 2

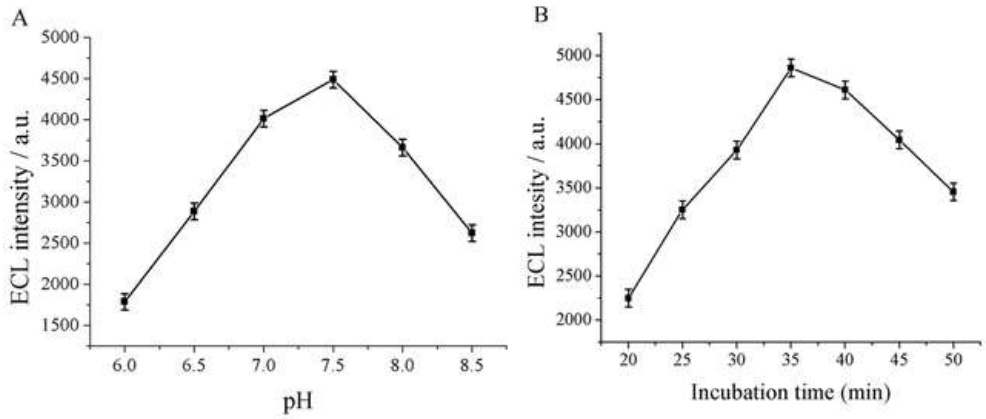

Fig. 3
55x23mm (300 x 300 DPI)

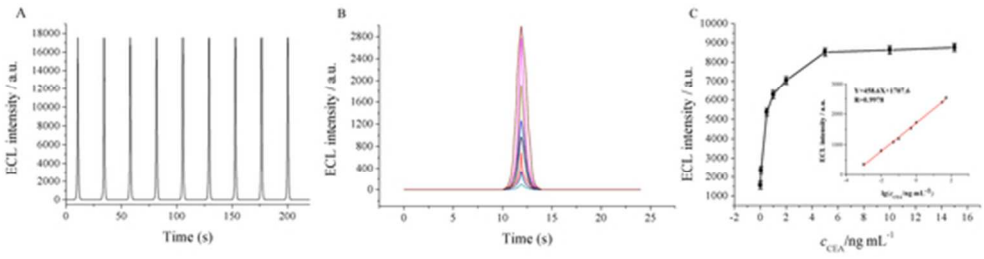

Fig. 4
50x12mm (300 x 300 DPI)

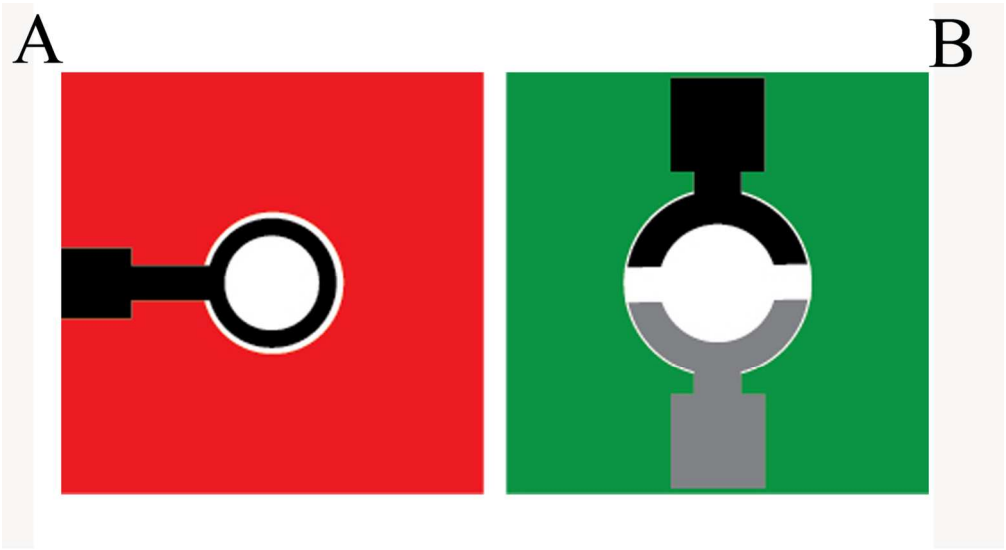

Scheme 1
127x69mm (300 x 300 DPI)

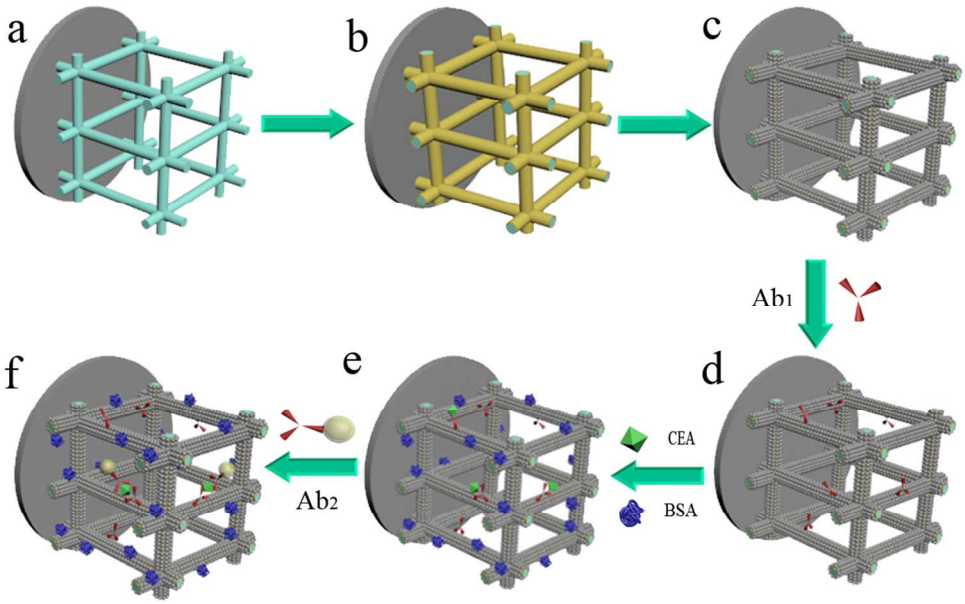

Scheme 2
102x63mm (300 x 300 DPI)

Table 1. Detection results of serum samples by the proposed and reference method.

Method	Sample			
	1 #	2 #	3 #	4 #
Proposed method detection result (ng mL^{-1})[a]	33.2	40.5	28.9	20.6
Reference method (ng mL^{-1})[a]	32.3	39.2	27.5	21.6
Relative deviation (%)	2.8	3.32	0.51	-4.6

[a]The average value of ten successive determinations.